High resolution x-ray diffraction analysis of InGaAs/InP superlattices

D. M. Cornet and R. R. LaPierre[a)]
Centre for Emerging Device Technologies, McMaster University, Hamilton, Ontario L8S 4L7, Canada

D. Comedi
Consejo Nacional de Investigaciones Científicas y Técnicas, Laboratorio de Física del Sólido, Departamento de Física, Facultad Ciencias Exactas y Tecnología, Universidad Nacional de Tucumán, 4000 Tucumán, Argentina

Y. A. Pusep
Instituto de Fisica de São Carlos, Universidade de São Paulo, 13560-970 São Carlos, Sao Paulo, Brazil

(Received 10 February 2006; accepted 14 July 2006; published online 25 August 2006)

The interfacial properties of lattice-matched InGaAs/InP superlattice (SL) structures grown by gas source molecular beam epitaxy were investigated by high resolution x-ray diffraction (HRXRD). SLs with various periods were grown to determine the contributions of the interface layers to the structural properties of the SLs. The HRXRD curves exhibited a number of features indicative of interfacial layers, including weak even-order satellite peaks, and a zero-order diffraction peak that shifted toward lower diffraction angles with decreasing SL period. A detailed structural model is proposed to explain these observations, consisting of strained InAsP and InGaAsP monolayers due to the group-V gas switching and atomic exchange at the SL interfaces. © *2006 American Institute of Physics*. [DOI: 10.1063/1.2335689]

I. INTRODUCTION

InGaAs/InP multiple quantum wells and superlattices (SLs) have numerous optoelectronic applications including semiconductor photodiodes, light sources, and modulators. InGaAs/InP heterostructures are also a model system for understanding semiconductor growth processes where mixed group-III and group-V interfaces are involved. The growth of nominally lattice-matched InGaAs/InP heterostructures and SLs grown by chemical beam epitaxy (CBE), metal organic vapor phase epitaxy (MOVPE), or molecular beam epitaxy (MBE) has therefore been investigated by numerous authors,[1–10] and a number of widely varying growth models have been developed.

During the gas-switching phase of InGaAs/InP heterostructure growth, there is an exchange of group-V atoms across the interface. This exchange results in changes to the structural properties of SLs or multiple quantum well structures. Benzaquen *et al.*,[1] for example, developed a CBE growth model with 3 ML (ML denotes monolayer) of $InAs_{0.75}P_{0.25}$ at the InGaAs-on-InP interface and 2 ML of $In_{0.52}Ga_{0.48}As_{0.21}P_{0.79}$ at the InP-on-InGaAs interface. In another CBE study, McKay *et al.*[4] arrived at a similar result, with a 5 Å $InAs_{0.65}P_{0.35}$ layer at the InGaAs-on-InP interface and a 5 Å $In_{0.532}Ga_{0.468}As_{0.2}P_{0.8}$ layer at the InP-on-InGaAs interface. Finally, a larger interfacial effect has been proposed by Sherwin *et al.*,[5] which involves an interfacial region of ~5 ML of $In_{0.75}Ga_{0.25}As_{0.5}P_{0.5}$.

InGaAs/InP SLs grown by MOVPE have also been reported with 2–3 ML of InGaAsP at the InP-on-InGaAs interface and 2–4 ML of InAsP at the InGaAs-on-InP interface due to As/P exchange.[6,7] Krost *et al.*[3] suggested that only a fraction of a monolayer of InAs is created during the gas switching from PH_3 to AsH_3 after completion of the InP layer and that a fraction of a monolayer of $In_{0.4}Ga_{0.6}As_{0.704}P_{0.296}$ is created at the inverted interface to create the strain balance necessary to fit their x-ray diffraction (XRD) rocking curves.

In SLs grown by MBE, Vandenberg *et al.*[8] performed an analysis using a kinematical diffraction step model which suggested that interfacial compositional deviations occur over less than 1 ML. As will be shown, this is not believed to be the case in the structures studied in this article. In another article by the same authors,[9] the presence of a 9 Å thick layer of $In_{0.53}Ga_{0.47}As_{0.985}P_{0.015}$ at the InP-on-InGaAs interface is reported due to substitution of P for As in the $In_{0.53}Ga_{0.47}As$ layer during growth interruption. This larger interfacial region is reinforced by Shiau *et al.*[10] who suggested the presence of 4 ML of compositionally graded InAsP at the InGaAs-on-InP interface.

This article reports a comprehensive high resolution (HRXRD) study in which an alternative interface model is proposed for InGaAs/InP SLs prepared by gas source MBE (GSMBE). This model accounts for grading in the interfacial layers and is shown to be valid over a range of superlattice periods.

II. EXPERIMENTAL DETAILS

The samples studied in this work were lattice-matched $In_{0.532}Ga_{0.468}As$/InP SL structures grown by GSMBE in which the InP barrier and InGaAs well layers were of equal thickness. Samples were grown with nominal SL periods ranging from 36 to 400 Å, corresponding to a range of 12–136 ML, with 1 ML defined as one layer of group-III atoms and one layer of group-V atoms. The structures were all grown with 30 periods of InGaAs/InP with the exception of the 400 Å sample which was grown with 20 periods.

[a)]Electronic mail: lapierr@mcmaster.ca

The growth times required to achieve each nominal layer thickness were determined by stylus profilometry measurements on previous thick-layer (3000–4000 Å) calibration samples. The In/Ga flux ratios required for lattice matching of the InGaAs layers to InP were established by (004) double crystal HRXRD rocking curves on the same thick-layer calibration samples. Based on these measurements, the lattice mismatch of the InGaAs layers is expected to be less than 0.02%.

All samples were grown on (001) *n*-type or semi-insulating InP substrates at a temperature of 465 °C. In GSMBE, the group-V constituents are supplied primarily in the form of As_2 and P_2 from the pyrolysis of AsH_3 and PH_3 in a dual filament cracker operating at 950–1000 °C. Throughout growth, the In flux rate remained constant corresponding to an InP growth rate of 0.532 μm/h and a V/III flux ratio of 2.0. The growth of the InGaAs layer occurred at a total growth rate of 1.0 μm/h and a V/III flux ratio of 1.5. Switching of the molecular beams at the InGaAs-on-InP interface occurred by first shuttering the In beam to terminate growth of the InP layer, initiating AsH_3 flow, terminating PH_3 flow, waiting 30 s, and then opening the In and Ga shutters to initiate growth of the InGaAs layer. Similarly, molecular beam switching at the InP-on-InGaAs interface occurred by first shuttering the In and Ga beams to terminate growth of the InGaAs layer, initiating the PH_3 flow, terminating the AsH_3 flow, waiting 30 s, then reopening the In shutter.

After growth, the SLs were characterized by HRXRD. Rocking curves of the (004) reflection were produced using the Bede D1 system in the four-reflection arrangement. Each SL structure was determined by comparing the measured rocking curves to simulated curves based on our interface model explained below. The simulated curves were obtained by using the Bede RADS Mercury (version 3.88) x-ray rocking curve software[11] based on the Takagi-Taupin equations of dynamical diffraction theory. The parameters of the model were varied systematically until agreement was obtained between the simulated and the measured rocking curves.

III. RESULTS

The measured HRXRD rocking curves shown in Fig. 1 exhibit the usual satellite peaks (order $n=\pm1,\pm2,\ldots$) centered around the average composition peak (order $n=0$). The angular separation between the satellite peaks is given by[12]

$$2\Lambda(\sin\theta_n - \sin\theta_o) = \pm n\lambda, \tag{1}$$

where Λ is the period of the SL (equal to the combined thickness of one InP and one InGaAs layers), θ_n is the diffraction angle for order n, θ_o is the angle for the zero-order ($n=0$) peak, and λ is the Cu $K\alpha$ x-ray wavelength of 1.541 Å. The SL periods determined from Eq. (1) are summarized in Table I.

In the sample with $\Lambda=400$ Å, the average composition peak can just be resolved from the substrate layer peak in Fig. 1, indicating a slight compressive strain of 0.012%. It is also observed in Fig. 1 that the splitting of the zero-order satellite peak from the substrate peak increases with decreasing period of the SL. These splittings are plotted in Fig. 2 versus the SL period. A lack of abrupt interfaces can explain the trend demonstrated by the solid line in Fig. 2, which is a theoretical fit to the data using the structural model (model 2-1) discussed below. Another notable feature present in Fig. 1 is the weak intensity of the even-order satellite peaks, providing further evidence of nonabrupt interfaces in the SL structure. For a perfectly abrupt interface, the even-order satellite peaks are expected to be absent.

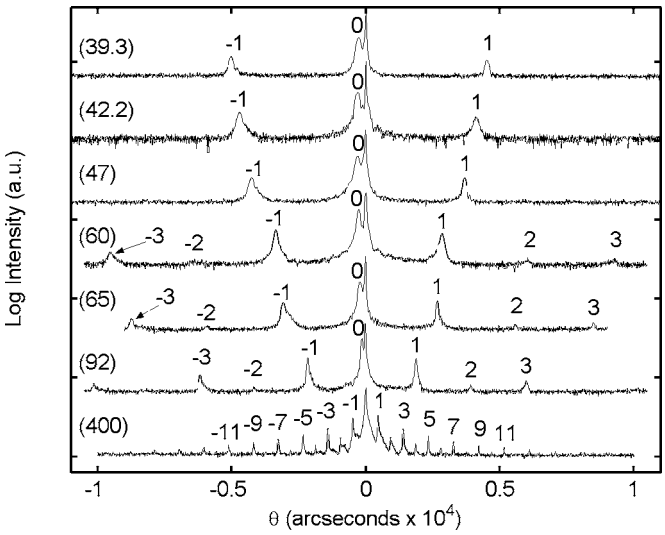

FIG. 1. Measured HRXRD (004) rocking curves. The measured SL period is indicated for each rocking curve in units of angstroms. Satellite orders are labeled, and the curves are offset for visual clarity.

IV. DISCUSSION

HRXRD curves were simulated for different interface models and compared to the measured curves. The general model, shown in Fig. 3, represents all five of the models considered. Previous work has shown that the phosphorous-terminated InP barrier layer in Fig. 3(a) can have a large portion of its final atomic layer replaced by arsenic during the gas-switching phase of growth.[13] The value y_{1a} indicates the fraction of atomic P replaced by As in the top group-V layer of the InP surface at the InGaAs-on-InP interface (interface 1). A second interface layer with As composition

TABLE I. Simulation results for the 2-1 model. Note that y_{2b} is fixed at 1.

	Interface 1 (InGaAs on InP)				Interface 2 (InP on InGaAs)	
Measured period (Å)	y_{1a} best fit	y_{1a} range	y_{1b} best fit	y_{1b} range	y_{2a} best fit	y_{2a} range
39.3	0.98	0.96–1	0.43	0.39–0.47	0.04	0.02–0.06
42.2	1.00	0.98–1	0.53	0.51–0.55	0.02	0–0.04
47	1.00	0.95–1	0.44	0.40–0.48	0.14	0.09–0.19
60	1.00	0.83–1	0.56	0.41–0.71	0.08	0–0.23
65	0.97	0.91–1	0.58	0.52–0.64	0.05	0–0.20
92	1.00	0.87–1	0.54	0.41–0.67	0.00	0–0.12
400	0.86	0.16–1	0	0–0.7	0.32	0–0.87

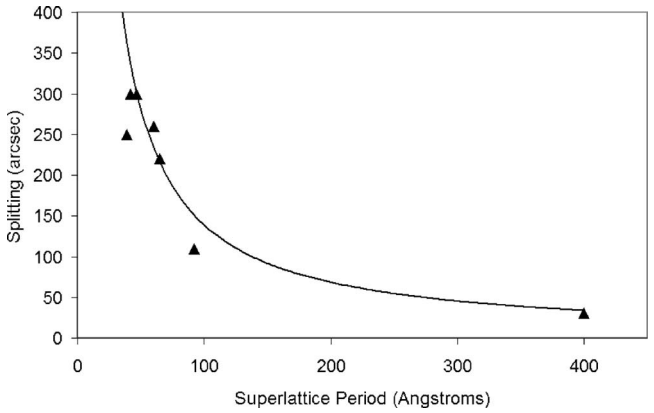

FIG. 2. Zero-order peak splitting vs superlattice period for measured (triangles) and simulated (solid line) data.

given by y_{1b} is introduced to account for the possible deeper penetration of As into an underlying group-V atomic layer. Similarly, y_{2a} and y_{2b} in Fig. 3(b) indicate the atomic fraction of As at the InP-on-InGaAs interface (interface 2). The resulting interface layer compositions used in the HRXRD simulations are indicated to the right in Figs. 3(a) and 3(b).

Due to the switching of both the group-III and group-V compositions at each interface, an intrinsic strain is present in the structure.[8] This strain is present even in the case of perfect lattice matching of the InGaAs wells to the InP barriers, and no group-III or -V atomic exchange across the interfaces ($y_{1a}=0$, $y_{1b}=0$, $y_{2a}=1$, $y_{2b}=1$), as illustrated in Fig. 4. Due to the sharing of the group-V atomic layers by the adjacent group-III layers, there exists 1 ML of $In_{0.532}Ga_{0.468}As_{0.5}P_{0.5}$ at interface 1 and 1 ML of $InAs_{0.5}P_{0.5}$ at interface 2. From a weighted average of the end member

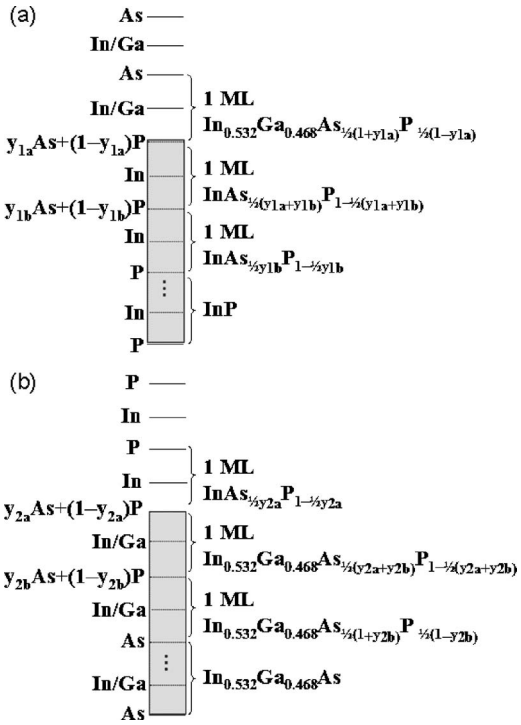

FIG. 3. Structural model for (a) interface 1 (InGaAs on InP) and (b) interface 2 (InP on InGaAs).

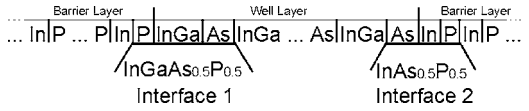

FIG. 4. Interface layers of a perfect InGaAs/InP SL structure.

lattice parameters, the lattice parameter of $InAs_{0.5}P_{0.5}$ is 5.9635 Å, and the lattice parameter of $In_{0.532}Ga_{0.468}As_{0.5}P_{0.5}$ is 5.7708 Å, resulting in a compressive strain of 1.62% and a tensile strain of 1.67% in these layers, respectively. It is assumed that this strain is confined to the interfaces and not graded through the surrounding layers.

Simulated HRXRD rocking curves of the structure in Fig. 4 are shown in Fig. 5, using the measured period for each sample from Table I. The observed zero-order peak splitting of the measured curves does not appear using this model. Also, the weak even-order satellite peaks in Fig. 1 are absent in the simulated curves of Fig. 5. It is therefore necessary to use the more general model of Fig. 3 to explain the HRXRD measurements.

Before running the simulation fitting routine it was necessary to find appropriate values for the fixed parameters, which are the In and Ga composition for the InGaAs wells, and the superlattice period. Based on previous thick-layer InGaAs calibrations, the In content of each InGaAs well was estimated to deviate by less than 0.3% from the lattice-matched value of 0.532. This was confirmed by the negligible splitting of the average composition peak from the substrate peak in the HRXRD curve for the $\Lambda=400$ Å SL. This made it reasonable to fix the In content of the wells at 0.532 for the simulations. Negligible exchange of group-III atoms at the interfaces was assumed due to the high sticking coefficients of these elements under the growth conditions used in this work.[14]

The thicknesses of the interfacial monolayers were estimated from an average of the end member composition lattice parameters. It was found, upon further analysis, that small changes ($\leqslant 0.1$ Å) in the thickness of these interfacial

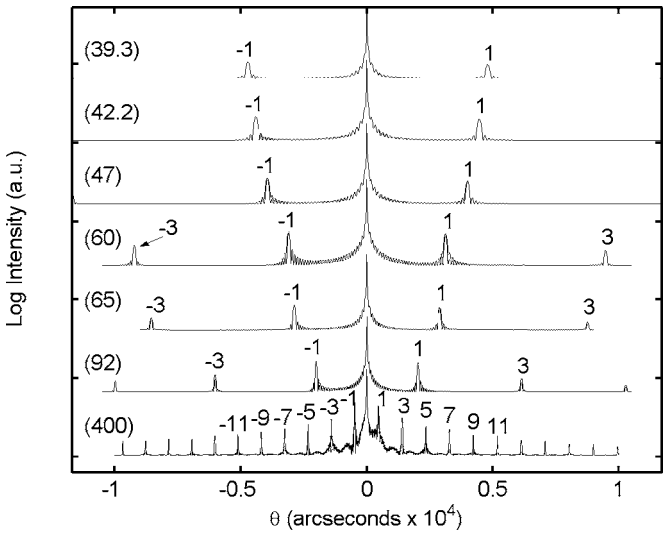

FIG. 5. Simulated HRXRD rocking curves of the SL structure illustrated in Fig. 4. The measured SL period is indicated for each rocking curve in units of angstroms.

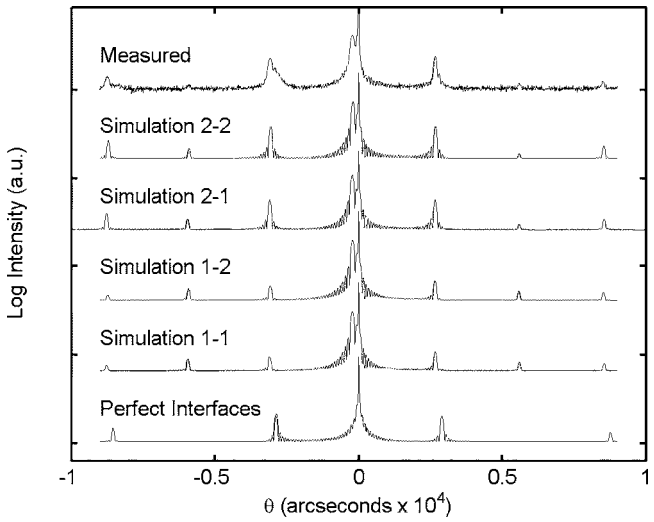

FIG. 6. Measured and simulated (004) HRXRD rocking curves for the Λ =65 Å rocking curve.

layers due to biaxial strain had little effect on the simulated curves, thus confirming the appropriateness of the estimated values. With the thickness of the interfaces and the InGaAs layer composition fixed as explained above, an appropriate thickness of the well/barrier layers was found by manually adjusting the SL period to match the satellite peak spacings in the experimental data. The resulting periods, shown in Table I, are the same as those determined by Eq. (1). In terms of thickness, the InP and InGaAs layers were each assumed to equal half the SL period.

The models were labeled using the notation 1-1, 1-2, 2-1, and 2-2, the first number indicating the number of mixed group-V monolayers in the InP layer at interface 1, and the second number indicating the number of mixed group-V monolayers in the InGaAs layer at interface 2. For the models with only one mixed monolayer at interface 1, y_{1b} was fixed at 0. Likewise, for the models with only one mixed monolayer at interface 2, y_{2b} was fixed at 1.

Figure 6 shows all four simulated curves compared to the measured curve for a representative sample. To emphasize the need for group-V atomic exchange at the interfaces, a simulation of the perfect interface structure of Fig. 4 is also included. Note that the satellite peak positions of the perfect interface model in Fig. 6 do not match those of the measured rocking curves due to the absence of splitting between the substrate and zero-order peak in the perfect interface model. Also, it can be seen that the 1-1, 1-2, and perfect interface models have insufficient peak intensities to fit the measured curves. This observation is clarified in Fig. 7, in which peak intensities are plotted as a function of peak order for several SL samples. It is clear that the solid lines representing the 2-1 and 2-2 models provide an improved fit to the experimental peak intensity data points compared to the dotted lines representing the 1-1 and 1-2 models.

A good fit to the measured peak intensities can be obtained with the 2-1 model, providing evidence of a partial substitution of P with As in the last two monolayers of the InP barrier. Only a slight improvement is observed in the 2-2 model. Based on the fact that As-for-P exchange is preferred

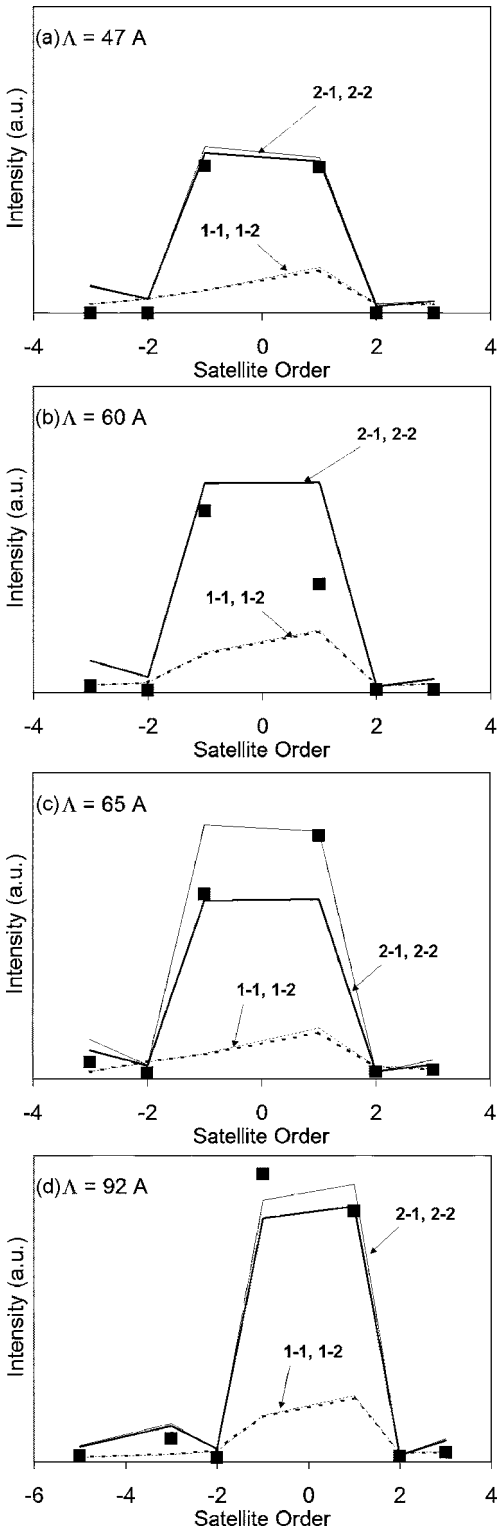

FIG. 7. Comparison of peak intensities for samples of period (a) 47 Å, (b) 60 Å, (c) 65 Å, and (d) 92 Å for each of the models. The solid lines represent the 2-1 (thick line) and 2-2 (thin line) models, and the dashed lines represent the 1-1 (thick dashed) and 1-2 (thin dashed) models. The experimental peak intensities are shown as square data points.

to P-for-As exchange,[14] significant P-for-As exchange in an underlying layer may be unlikely. Therefore, the negligible improvement in the 2-2 simulated curve is not a compelling evidence to support a model with a multilayer P-for-As exchange at interface 2. Thus, it is believed that the 2-1 model best describes the structures.

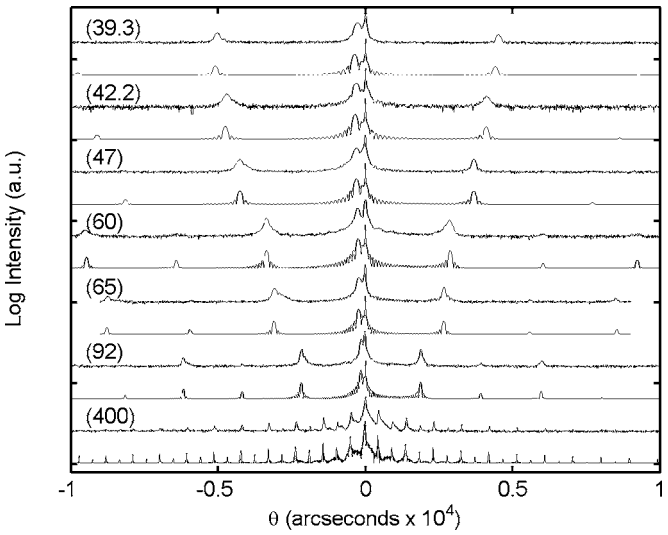

FIG. 8. Experimental and simulated rocking curves using the same model and interface layer compositions ($y_{1a}=1$, $y_{1b}=0.5$, $y_{2a}=0.1$, and $y_{2b}=1$) for each sample. The curves are shown offset for visual clarity with the experimental curve above the simulated curve for each sample. The measured SL period is indicated for each sample in units of angstroms.

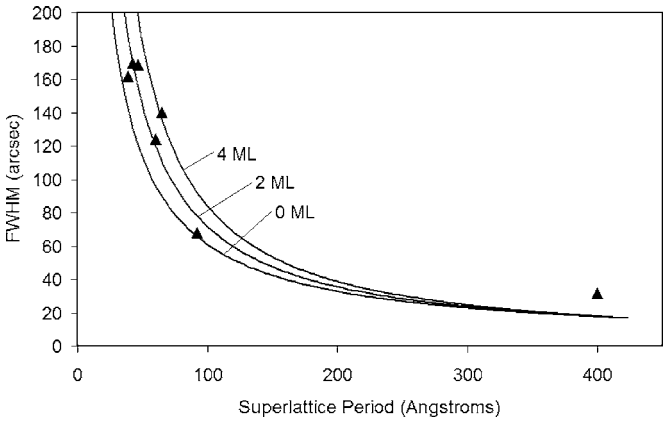

FIG. 9. Measured (triangles) and simulated (solid lines) FWHM of the $n=-1$ satellite peak for each sample. Simulated lines based on 0, 2, and 4 ML of interface roughness are shown.

The compositions of the interface layers, as determined by fitting the 2-1 model to the experimental HRXRD curves, are shown in Table I. For all samples the y_{1a} values are close to unity. This indicates that the top atomic layer of P in each InP barrier is completely replaced by As. The fact that the optimized y_{1b} value is approximately 0.5 on average indicates that about half of the P in the underlying layer is replaced by As. At interface 2 the value of y_{2a} for the 2-1 model was found to be about 0.1 on average indicating that almost all ($\sim 90\%$) of the As at the top interfacial layer is replaced by P.

The sensitivity of the model parameters (y_{1a}, y_{1b}, and y_{2a}) on the "goodness of fit" was estimated by consecutively varying each parameter until the shift in the average composition peak exceeded the substrate full width at half maximum (FWHM). This provided a range of the interface compositions, shown in Table I, within which a "good fit" of the model to the experimental rocking curves was still obtained. Note that for the 2-1 model the value of y_{2b} is fixed at 1. The relative insensitivity displayed by the $\Lambda=400$ Å sample may be attributed to the almost negligible thickness of the interface layers in comparison to the SL period in this sample.

From the interface compositions in Table I, parameter values were chosen ($y_{1a}=1$, $y_{1b}=0.5$, $y_{2a}=0.1$, and $y_{2b}=1$) and substituted into the Fig. 3 model to create simulated HRXRD curves using consistent interface compositions for all of the samples. These simulations are shown in Fig. 8 and compared to the measured curves for each sample.

Figure 8 shows excellent agreement between the measured and simulated curves. Firstly, the position of the zero-order peak as a function of SL period is reproduced in Fig. 2. This feature is due to the effect of the additional As in the InP interfacial layers (interface 1) causing the average composition peak to shift further into compressive strain for the shorter period SLs where the interfacial layers constitute a larger fraction of the total period. Secondly, the intensities of the measured and simulated SL peaks are in excellent agreement, including the weak even-order peaks.

Figure 9 compares the measured and simulated FWHM vs SL period for each of the samples studied. The simulated curve labeled 0 ML indicates the FWHM obtained from the 2-1 model results of Fig. 8. A deviation between the simulated FWHM (0 ML curve) and the measured data is evident for the small period SLs where no interface roughness effects are considered. The influence of interface roughness on the FWHM was estimated by simulating the angular shift in the $n=-1$ satellite peak due to changes in SL period of 2 and 4 ML, as indicated in Fig. 9. The 2 ML interface roughness line provides the best fit to the experimental data. The origin of this roughness may be partially attributed to the y_{1b} and y_{2a} layers of the 2-1 interface model. The y_{1a} and y_{2b} layers of the 2-1 model, both with full As coverage on average, are unmixed and would therefore not contribute to the roughness. Further evidence of interface roughness has been provided by Raman spectroscopy measurements on these samples as reported elsewhere.[15]

In terms of the consistency in the period of the SLs, the quality is quite good. This is apparent from the small amount of satellite peak broadening that occurs with increasing satellite order. A quantitative analysis of the peak broadening for the $\Lambda=400$ Å sample shows that the FWHM of the satellite peaks increased by only about 1.5 arc sec with each consecutive order. Clear broadening with increasing satellite order is a sign of significant variations in the SL period.[16] When compared to data from other studies[17] the variation in the SL period can be estimated at about 0.3% (~ 0.5 ML).

Our analysis thus far has assumed no As carryover into the InP barriers after growth of each InGaAs well. However, the presence of graded $InAs_yP_{1-y}$ layers has been suggested by a number of authors.[18–20] To determine the influence of this effect, we replaced the single interface layer of $InAs_{1/2y_{2a}}P_{1-1/2y_{2a}}$ and the subsequent InP monolayers of each barrier layer in our previous model with an exponential As tail along the growth direction as described by

$$y_m = y_o e^{-\beta(m-1)}, \tag{2}$$

where y_m is the fractional As content of monolayer m ($m=1,2,\ldots$), y_0 describes the initial As content, and β is a constant describing the composition gradient. A y_o value of 0.06 and a β value of 0.077 provided some improvement to the fit of the experimental data. Thus, the composition of the first InAsP monolayer ($m=1$) in this model was 0.06, as compared to 0.05 ($=1/2y_{2a}$) on average for the previous model.

During growth of the InGaAs well, a fraction of the available In can segregate to the growth front.[21] To model this effect, the indium content (x_m) of each monolayer m ($m=1,2,\ldots$) of InGaAs in the previous model was allowed to vary according to

$$x_m = 0.532(1 - R^m), \tag{3}$$

where R is a constant describing the composition profile.[21] The best results were achieved with an R value of 0.0078. Thus, simulations allowing for this effect suggested that there was no significant In segregation in the samples investigated in this study.

The gradient model provided a slightly improved fit of the simulated HRXRD curves to the experimental satellite peak intensities. Complementary studies, including characterization by photoluminescence, transmission electron microscopy, and secondary ion mass spectrometry are currently underway to further support these results.

V. CONCLUSIONS

HRXRD studies of InGaAs/InP SLs have suggested an interface model in which complete exchange of P with As in the top monolayer, and partial ($\sim 50\%$) exchange in the second monolayer, occurs in the InP layer for growth of InGaAs on InP. In the case of InP on InGaAs, about 90% exchange of As with P occurs in the top monolayer of InGaAs with no exchange in the underlying monolayers. Surface roughness was estimated to be ~ 2 ML.

ACKNOWLEDGMENTS

The authors would like to thank the Natural Sciences and Engineering Research Council of Canada, FAPESP, and CNPq for financial support.

[1] R. Benzaquen, A. P. Roth, and R. Leonelli, J. Appl. Phys. **79**, 2640 (1996).
[2] J. M. Vandenberg, A. T. Macrander, R. A. Hamm, and M. B. Panish, Phys. Rev. B **44**, 3991 (1991).
[3] A. Krost, J. Bohrer, H. Roehle, and G. Bauer, Appl. Phys. Lett. **64**, 469 (1994).
[4] H. A. McKay, R. M. Feenstra, P. J. Poole, and G. C. Aers, J. Cryst. Growth **249**, 437 (2003).
[5] M. E. Sherwin, F. L. Terry, G. O. Munns, J. S. Herman, E. G. Woelk, and G. I. Haddad, J. Electron. Mater. **21**, 269 (1992).
[6] L. Francesio, P. Franzosi, and G. Landgren, J. Phys. D **28**, A169 (1995).
[7] J. Camassel, J. P. Laurenti, S. Juillaguet, F. Reinhardt, K. Wolter, H. Kurz, and D. Grutzmacher, J. Cryst. Growth **107**, 543 (1991).
[8] J. M. Vandenberg, M. B. Panish, R. A. Hamm, and H. Temkin, Appl. Phys. Lett. **56**, 910 (1990).
[9] J. M. Vandenberg, S. N. G. Chu, R. A. Hamm, M. B. Panish, and H. Temkin, Appl. Phys. Lett. **49**, 1302 (1986).
[10] G. J. Shiau, C. P. Chao, P. E. Burrows, and S. R. Forrest, J. Appl. Phys. **77**, 201 (1995).
[11] Bede Scientific Instruments Ltd., Bowburn South Industrial Estate, Bowburn, Durham, England.
[12] D. K. Bowen and B. K. Tanner, *High Resolution X-ray Diffractometry and Topography* (Taylor & Francis, Landan, 1998), pp. 141–142.
[13] B. Lakshmi, B. J. Robinson, D. T. Cassidy, and D. A. Thompson, J. Appl. Phys. **81**, 3616 (1997).
[14] R. R. LaPierre, B. J. Robinson, and D. A. Thompson, J. Appl. Phys. **79**, 3021 (1996).
[15] Y. A. Pusep, A. G. Rodrigues, J. C. Galzerani, D. M. Cornet, D. Comedi, and R. R. LaPierre, Phys. Rev. B **73**, 235344 (2006).
[16] W. J. Bartels, *Thin Film Growth Techniques for Low-Dimensional Structures* (Plenum, New York, 1987), Vol. 163, pp. 441–458.
[17] W. J. Bartels, J. Hornstra, and D. J. W. Lobeek, Acta Crystallogr. **42**, 539 (1986).
[18] W. Seifert, X. Liu, and L. Samuelson, Appl. Phys. Lett. **62**, 949 (1993).
[19] H. J. Chen, R. M. Feenstra, P. G. Piva, R. D. Goldberg, I. V. Mitchell, G. C. Aers, P. J. Poole, and S. Charbonneau, Appl. Phys. Lett. **75**, 79 (1999).
[20] T. Mozume, H. Kashima, K. Hosomi, K. Ouchi, H. Sato, H. Masuda, T. Tanoue, and I. Ohbu, J. Vac. Sci. Technol. B **13**, 276 (1995).
[21] K. Muraki, S. Fukatsu, Y. Shiraki, and R. Ito, Appl. Phys. Lett. **61**, 557 (1992).